Experimental and Theoretical Analysis of Photoinduced Electron Transfer: Including the Role of Liquid Structure

S. F. Swallen, Kristin Weidemaier, H. L. Tavernier, and M. D. Fayer*

Department of Chemistry, Stanford University, Stanford, California 94305

Received: November 30, 1995; In Final Form: February 22, 1996[⊗]

Experimental determinations of the dynamics of photoinduced electron transfer from rubrene to duroquinone in three solvents, dibutyl phthalate, diethyl sebacate, and cyclohexanone are presented. Measurements of the donor (rubrene) fluorescence decays were made with time-correlated single-photon counting. The data are analyzed using recent theoretical developments that include important features of the solvent, i.e., the effects of finite molecular volume on local solvent structure and on the mutual donor−acceptor diffusion rates. Inclusion of the liquid radial distribution function (rdf) in the theory accounts for the significant variation of the acceptor concentration near a donor. Because the concentration of acceptors near a donor is substantially greater than the average concentration used in a featureless continuum liquid model, incorporating the rdf is necessary to properly analyze experimental data. Hydrodynamic effects, which slow the rate of donor−acceptor approach at short distance, are important and are also included in the theoretical analysis of the data. The data analysis depends on a reasonable model of the rdf. A hard-sphere liquid rdf is shown to be sufficiently accurate by comparing model electron-transfer calculations using a hard-sphere rdf and an rdf from neutron-scattering experiments reported in the literature. A method is presented to obtain the hard-sphere parameters needed to calculate the rdf. The method uses a self-consistent determination of the hard-sphere radius and diffusion constant and the solvent self-diffusion constant calculated from the Spernol and Wirtz equation. The Marcus form of the distance-dependent transfer rate is used. For the highest viscosity solvent (dibutyl phthalate), a unique set of the Marcus transfer parameters is obtained. For lower viscosity solvents, the transfer parameters are less well defined, but information on the distance and time dependence of charge separation is still acquired. These experiments, combined with the theoretical analysis, yield the first realistic description of through-solvent photoinduced electron transfer.

I. Introduction

Because of its ubiquitous role in chemical processes, electron transfer has been the focus of a great deal of research in recent years. The goal has been to obtain an understanding of the spatial and temporal dependences of intramolecular and intermolecular electron-transfer. Photoinduced charge separation is of particular interest due to its importance in photosynthesis, photochemical reactions, and technical applications. In addition, the initiation of the electron-transfer process by a fast light pulse enables dynamical studies to directly examine the kinetics of electron transfer. To complement a variety of experimental studies,[1−10] a number of theoretical descriptions have been developed to predict the rates of photoinduced charge separation.[11−26] Some success has been achieved in describing intramolecular photoinduced electron transfer for systems in which a donor and a single acceptor are held at fixed distance.[16,27−29] However, in systems where through-solvent intermolecular transfer is observed, the situation is more complex. In liquid solutions, a donor can interact with many acceptors, and the rates of reaction are influenced by the distribution and diffusion of the donors and acceptors.

It has been observed that the rate of quenching of a photoexcited donor molecule by electron transfer to an acceptor is significantly increased as the viscosity of the solvent is decreased.[4,30] This indicates the importance of diffusion for the kinetics of electron transfer. For donor−acceptor electron-transfer reactions under the influence of diffusion, modeled as a three-level system—a donor with acceptors in their ground states (DA), the donor in the photoexcited state (D*A), and the donor and an acceptor in the charge-transfer state (D^+A^-)—an exact solution to the time-dependent state probabilities has been obtained.[22−24] Previous attempts to fit experimental data using this statistical mechanical theory have met with a fair degree of success.[4,31,32] However, until recently the theory made simplifying assumptions about the physical characteristics of the solution being studied. As with other less detailed theoretical methods which have been applied to photoinduced electron transfer in solution, the influential effects of the solvent structure were ignored. The donor and acceptor molecules were assumed to be diffusing in a structureless continuum which interacts with the particles only through the dielectric properties and the reorganization energy of the solvent.[4,16,33] However, it has been shown recently[34] that this assumption can lead to significant errors in the analysis of electron-transfer data. By ignoring the finite size of the solvent molecules, fundamental properties of liquids, which play a key role in electron-transfer dynamics, were not included in the theory.

The nonzero volume of the solvent molecules surrounding the donor and acceptor has been shown to affect the rates of electron transfer in two distinct manners. The first of these is the result of short-range repulsion due to the finite volume of all molecules. This interaction leads to variations in local solvent density about each particle in solution. Because real molecules are not able to overlap and thus cannot pack into a space-filling configuration, the distribution of particles about any point is radially nonuniform. Instead, the surrounding solution exhibits a decaying oscillation in particle density, centered about the bulk average density. A great deal of

[⊗] Abstract published in *Advance ACS Abstracts,* April 15, 1996.

S0022-3654(95)03583-0 CCC: $12.00

research spanning many decades has been done to study and model this effect, and accurate methods of calculating the two-particle radial distribution function, $g(R)$, have been known for many years.[35−38] Solvent structure has been shown theoretically to have a major effect on the rates of electron transfer in liquid systems.[34] On the relatively short-range distance scale of electron transfer, the major variations in local solvent structure strongly influence the distribution of acceptor molecules about each donor. Because the rates of through-solvent transfer are acutely distance dependent, these density variations can greatly affect the probability of quenching of an excited donor by electron transfer.

In addition to variations in local concentrations of acceptor molecules, the finite volume of the solvent molecules also strongly influences the rates of diffusion between a donor and surrounding acceptors. Studies of interparticle diffusion rates have demonstrated that these correlated motions are strongly dependent upon the radial separation between the two molecules at short distances.[39−43] As a pair moves toward contact, intervening solvent molecules can act as a barrier to closer approach, thus diminishing the rate at which the two converge. As a result, the value of the Fick diffusion coefficient is no longer a constant but is instead a distance dependent function $D(R)$. This phenomenon, known as the hydrodynamic effect, can play a significant role in the dynamics of electron transfer.[34] Diffusion brings acceptors within range of an excited donor, permitting electron transfer to occur. Since the hydrodynamic effect reduces the rate of approach of acceptors toward a donor, the dynamics of electron transfer are slowed considerably. This is particularly true at longer times. The short time dynamics are dominated by acceptors that are close to the donor at the time of excitation and are controlled by the initial local solvent structure. The high acceptor concentration close to a donor, created by the short-range solvent organization, greatly increases the rate of electron transfer at short time. However, for members of the ensemble of excited donors that do not have acceptors close by at the time of excitation, interparticle diffusion plays a significant role in the time-dependent dynamics. Due to a decrease in the rates of close approach between donors and acceptors, the hydrodynamic effect lessens the ensemble-averaged probability of electron transfer when compared to theoretical calculations that do not include it. Therefore, both the solvent structure and the hydrodynamic effect, which result from the molecular nature of the liquid, must be included in a realistic description of photoinduced electron transfer in liquids.

A recent theoretical study has successfully included both the solvent structure $g(R)$ and the hydrodynamic effect $D(R)$ in the statistical mechanical theory of electron transfer.[34] This current work uses the new theoretical results for the first time to analyze experimental data in a manner that includes the important aspects of liquid properties. In the experiments, photoinduced electron transfer is studied by observing the time dependence of donor fluorescence with time-correlated single-photon counting. The donor, rubrene (RU), and electron acceptor, duroquinone (DQ), have been examined in several solvents of varying viscosity and dielectric properties. Using the Marcus form of the distance-dependent transfer rate constant and a least-squares fitting algorithm, successful fits to the fluorescence quenching observables in three solvents are presented. This is the first attempt to determine the Marcus electron-transfer parameters, J_0 and β, by including a full description of solvent structure and diffusional effects. These parameters represent the magnitude of the transfer matrix element at contact and the spatial extent of the molecular wave function overlap, respectively. The values of these electron-transfer parameters determined in previous studies were skewed to account for the solvent effects $g(R)$ and $D(R)$ which were not included in the theoretical analysis.

The remainder of this paper is organized as follows: Section II provides the theoretical framework needed for analysis of the experimental data. It includes a discussion of the radial distribution function and the hydrodynamic effect and gives the key equations that are necessary for calculation of the observable excited state survival probability. Section III discusses the specific methods used to obtain system parameters such as the molecular hard-sphere radius, the mutual diffusion coefficient, and the solvent $g(R)$ function. Section IV presents experimental electron-transfer data and demonstrates the success and applicability of the theory.

II. Theory

Considerable work has been done previously to develop a theory which calculates the time-dependent probabilities of photoinduced forward electron transfer and back transfer (geminate recombination).[22−26,34] These expressions can be used to fit the time-resolved experimental observables of an intermolecular donor−acceptor charge-transfer system. The theory, which will be summarized below, produces an exact expression for $\langle P_{ex}(t)\rangle$, the ensemble-averaged probability that an initially photoexcited donor remains excited at time t after excitation for a given model of acceptor spatial distribution and diffusion coefficient. Until recently, all through-solvent models of charge transfer have assumed that the solvent is an unstructured continuum. As discussed in the Introduction, this can lead to significant errors in understanding the distance and time dependence of electron transfer.

The distance-dependent rate of electron transfer from the excited donor to any acceptor located a distance R away is given by $k_f(R)$. Several forms of $k_f(R)$ have been examined previously,[13,14,32] but the most commonly accepted form for moderately exothermic reactions is given by Marcus:[16,33]

$$k(R) = \frac{2\pi}{h\sqrt{4\pi\lambda(R)k_B T}} J_0^{\,2} \exp\left(\frac{-(\Delta G(R) + \lambda(R))^2}{4\lambda(R)k_B T}\right) \times \exp(-\beta(R - R_m)) \quad (1)$$

J_0 is the magnitude of the transfer matrix element at contact, and β is a measure of the through-solvent donor and acceptor wave function overlap. R_m is the contact distance between the donor and acceptor. The reorganization energy, $\lambda(R)$, is expressed as

$$\lambda(R) = \frac{e^2}{2}\left(\frac{1}{\epsilon_{op}} - \frac{1}{\epsilon_s}\right)\left(\frac{1}{R_d} + \frac{1}{R_a} - \frac{2}{R}\right) \quad (2)$$

where ϵ_{op} and ϵ_s are the optical and static solvent dielectric constants. R_d and R_a are the radii of the donor and acceptor. $\Delta G(R)$ is the free energy change associated with electron transfer. It can be obtained as a function of distance by experimentally measuring the redox potentials of the donor and acceptor and solving the Rehm−Weller equation:[44,45]

$$\Delta G(R) = -h\nu - \frac{e^2}{4\pi\epsilon_0\epsilon_s R} + \Delta\epsilon \quad (3)$$

where $h\nu$ is the energy of electronic S_0, $\nu_0 \rightarrow S_1$, ν_0 vertical excitation, ϵ_0 is the permitivity of free space, and $\Delta\epsilon = \epsilon^0(\text{donor,ox}) - \epsilon^0(\text{acceptor,red})$. $\epsilon^0(\text{donor,ox})$ and $\epsilon^0(\text{acceptor,red})$ are the oxidation and reduction potentials of the donor and acceptor.

The following subsections will present the theoretical material necessary to analyze the data presented below.

A. Solvent Structure, *g*(*R*). It is well-known that solvent molecules are not distributed randomly in condensed-phase solutions but instead exhibit a large degree of local structure.[39,46−48] This results in significant distance dependent fluctuations in the local density about any molecule, with the largest perturbations occurring at or near contact. These variations influence the time-dependent probabilities of electron transfer in two important ways. Foremost is the direct influence of changing the local density of acceptors about a donor. The local region near contact about any photoexcited donor is much more likely to be occupied by an acceptor molecule than would be expected if the solvent were approximated as a continuum. As the radial separation is increased, the solvent structure oscillates about the average value of the density, converging to the bulk average at long distances. For relatively dilute acceptors (a few tenths molar or less) the acceptor density variation follows the solvent density variation.[49] Mathematically, these density fluctuations can be accounted for by rewriting the particle distribution function as $p'(R) = g(R) \times p(R)$, where $p(R)$ is the isotropic, unstructured particle distribution, and $g(R)$ is the solvent structure radial distribution function (rdf). It should be noted that this probability distribution is strictly accurate only in the absence of acceptor−acceptor excluded volume. In this limit, the distribution function for each acceptor is independent of all others in solution. If the concentration of acceptor molecules is not too high (less than a few tenths molar), the multiparticle distribution function $p'(R)$ can be used with no loss of accuracy.[50]

The solvent structure additionally influences the long-term electron-transfer probabilities in a more subtle manner than altering the local particle concentration. Even though the individual particles in a liquid are in constant motion, the local structure, given by the radial distribution function $g(R)$, is a static function. For a particular solvent density, $g(R)$ is independent of time. Thus, while individual particles are allowed to diffuse in solution, the liquid structure must be preserved. In this manner, the solvent structure acts as a potential when solving eq 5, given below. For forward transfer, assuming initially neutral molecules, the effective potential due to the solvent structure can be included with a term $V(R) = -\ln[g(R)]$,[39,43] where $V(R)$ is the potential divided by kT. This "potential of mean force," as it has been called, was investigated by Northrup and Hynes.[43] They examined its influence on diffusion-controlled reactions occurring at molecular contact. This present work integrates the concept of solvent structure in the theory of electron transfer, and extends it to through-solvent reactions that are both thermodynamically and diffusion controlled. For the general case of initially charged molecules, the potential can be written to include a Coulombic attraction or repulsion: $V(R) = -\ln[g(R)] + R_c/R$, where R_c is the Onsager length. In this way, the correct initial and time-dependent positions of ionic or neutral molecules in diffusive systems can be taken into account.

B. Hydrodynamic Effect, *D*(*R*). Theoretical[41−43] and experimental[51,52] studies of fluid flow have shown that molecular interactions cause the rates of interparticle diffusion to be distance dependent. The mutual diffusion coefficient is found to depend on the radial separation between the molecules being studied. When two particles in solution are separated by a large distance, their diffusive motions do not influence each other, and the value of the Fick diffusion coefficient describing the motion between the pair approaches a limiting value, D. However, when two particles approach each other, their motions become correlated. In this case, the mutual diffusion coefficient must be written as a function of the radial separation, $D(R)$.[39,41−43] This hydrodynamic effect originates from the short-range repulsive interactions between particles. As a donor and acceptor diffuse toward each other, solvent molecules must vacate the intervening space. When the two approach contact, the available paths of escape for occluding molecules are decreased, thus lessening the probability that this action will occur. Due to this restriction, the interparticle diffusion coefficient is decreased substantially when two molecules are within a small separation distance. This is particularly true on the distance scale of electron transfer.

Previous studies have discussed a number of the theoretical approaches for this distance-dependent term,[39] investigating the accuracy and utility of each. The most common expression currently used is an approximate analytical form given by Northrup and Hynes:[43]

$$D(R) = D\left[1 - \frac{1}{2}\exp\left(\frac{R_m - R}{R_m}\right)\right] \tag{4}$$

R_m is the contact distance between the donor and acceptor molecules, and D is the value of the Fick diffusion coefficient at infinite separation. The impact of the hydrodynamic effect on electron-transfer calculations has been examined previously.[34] It is clear that a simple, distance-independent value for the diffusion coefficient is insufficient to realistically model liquid diffusion in the context of electron transfer.

C. Calculation of Physical Observables. The inclusion of local solvent structure and a distance-dependent diffusion coefficient requires modification of the previously presented statistical mechanical theory.[34] The two-particle survival probability is given by

$$\frac{\partial}{\partial t} S_{ex}(t|R_0) = L^+_{R_0} S_{ex}(t|R_0) - k_f(R_0) S_{ex}(t|R_0) \tag{5}$$

where R_0 is the initial donor−acceptor separation. The adjoint of the Smoluchowski diffusion operator, $L^+_{R_0}$, is required when the particles are diffusing in a potential. This operator is expressed as

$$L^+_{R_0} = \frac{1}{{R_0}^2} \exp(V(R_0)) \frac{\partial}{\partial R_0} D(R_0) {R_0}^2 \exp(-V(R_0)) \frac{\partial}{\partial R_0} \tag{6}$$

where $V(R_0)$ is the distance-dependent potential divided by kT felt by the diffusing acceptors. $D(R_0)$ is the diffusion coefficient, given by eq 4. Physically, the function $S_{ex}(t|R_0)$ represents the probability that a donor molecule, initially excited at time $t = 0$, is still in the excited state, given that an acceptor was located at distance R_0 at $t = 0$. With the constraints of the proper initial conditions and a reflecting boundary condition at contact, the solutions are obtained by integrating over all possible initial and final positions. These results give an analytical expression for the physically observable probability of remaining in the excited state at a time t after photoexcitation:[22,53]

$$\langle P_{ex}(t) \rangle = \exp(-t/\tau) \exp\left(-4\pi C \int_{R_m}^{\infty} [1 - S_{ex}(t|R_0)] {R_0}^2 g(R_0)\, dR_0\right) \tag{7}$$

where C is the concentration of acceptor molecules. The first exponential has been included to account for excited state decay due to fluorescent relaxation. This is the decay that will occur in the absence of electron transfer. Expressions for the two-particle survival probability, $S_{ex}(t|R_0)$, cannot be obtained

analytically. Instead, numerical solutions of eq 5 are calculated using the Crank−Nicholson finite differencing method.[54−56] Thus, by means of numerical integration, it is possible to obtain exact solutions to the time-dependent excited-state probability given a particular model of the spatial distribution of acceptors. With an appropriate form of the radial distribution function, $g(R)$, and solving eq 5 using a proper potential $V(R)$ and diffusion coefficient $D(R)$, an accurate form of $\langle P_{ex}(t)\rangle$ can be found.

III. System Parameters

To correctly model an experimental electron-transfer system and accurately calculate the excited-state probability, a number of system parameters must be obtained. The magnitude of the donor−acceptor mutual diffusion coefficient in each solvent plays a significant role in particle positions and electron-transfer dynamics and must be known accurately. The same is true for the characteristics of individual solvent and solute molecules. A hard-sphere model of the solvents will be shown to be sufficiently accurate to employ in the description of electron-transfer dynamics in liquids. The use of the hard-sphere model requires a choice of the hard-sphere diameter and thus the liquid packing fraction. This is an area which has been the focus of significant debate. A number of theoretical approaches have been presented which calculate molecular dimensions with varying degrees of accuracy.[57−60] In addition, once the molecular parameters have been obtained, an accurate form of the local solvent structure is required. This section presents the methods used to find sufficiently accurate values and forms of these parameters, as well as the efficacy and limitations involved.

A. Diffusion Coefficient. The choice of the large-separation value for the diffusion coefficient, D, is critical. Typically, studies of dynamics in liquids have used values for D calculated with the Stokes−Einstein equation.[4,32,39,61,62] However, theoretical and experimental studies have presented evidence that neutral solvated molecules diffuse at rates significantly different from the Stokes−Einstein predictions, due to solvation and Coulombic attraction effects.[63−66] Various approaches, mainly empirical studies of diffusion rates, have been used to describe diffusion of neutral molecules in solution more accurately. A well-accepted form of the diffusion equation which has been found to agree well with experimental measurements of neutral molecules is based upon a perturbation of the Stokes−Einstein equation:

$$D = kT/6\pi\eta r\, f_{sw} \tag{8}$$

where η is the solvent viscosity, and r is the molecular radius. The perturbative term f_{sw} is given by a semiempirical equation proposed by Spernol and Wirtz:[65,66]

$$f_{sw} = (0.16 + 0.4r_m/r_a)(0.9 + 0.4T_m^r - 0.25T_a^r) \tag{9}$$

r_m and r_a are the radii of the solute (m) and solvent (a), and T_x^r is the reduced temperature of the solute (x = m) and solvent (x = a). These temperatures describe the intermolecular interactions and are obtained from

$$T_x^r = \frac{T - T_x^f}{T_x^b - T_x^f} \tag{10}$$

T_x^f is the freezing point, and T_x^b is the boiling point of the appropriate specie. Equations 8−10 reproduce experimentally determined diffusion constants and yield values of D that are significantly greater than those obtained from the Stokes−Einstein equation. It should be noted that eqs 8−10 apply only to the diffusion of neutral molecules and are not an accurate description of ion motion. Other approaches for the determination of D can be used for the diffusion of ions.[63,67−69] The experiments presented below involve only neutral species and are thus well described by eq 8.

The experimental work presented here examines rubrene and duroquinone as the donor and acceptor diffusing in three organic solvents: dibutyl phthalate, diethyl sebacate, and cyclohexanone. Mutual diffusion coefficients in the three solvents were calculated from eq 8, using molecular radii obtained either from crystallographic data or from the method presented in section IIIB. Crystallographic data exist for both rubrene and duroquinone.[70,71] The donor and acceptor radii were found by obtaining the molecular volume from the crystal structure, scaling it by 74% to account for the closest packing of spherical particles and then determining the hard-sphere radius, $^4/_3\pi R^3$ that would reproduce this volume. This type of calculation for similar molecules generally overestimates the particle radius by ∼10%.[72] With this reduction factor, radii of 4.5 Å for RU and 3.4 Å for DQ are obtained, and these values were used in fits to the experimental data.

B. Self-Consistent Determination of Solvent Radii. To utilize the theoretical results presented in this work, a detailed knowledge of the solvent rdf is required. Ideally, neutron or X-ray scattering studies could provide experimentally determined radial distribution functions, $g(R)$. While there is a great deal of scattering data on condensed-phase systems, most is focused on solids or very simple liquids. Only a limited number of experiments have been performed on complex liquids, and thus data on solvent structure for most organic liquids are not available. Experimental $g(R)$ functions for the three solvents used in the experiments presented below are not available. Thus a theoretical method for determining $g(R)$ is required. One common approach is to use a hard-sphere potential, generating $g(R)$ from numerical solutions to the Percus−Yevick integral equation. Although other forms of the potential may be chosen, e.g., Lennard-Jones, it will be shown below that the hard-sphere $g(R)$ provides a sufficiently accurate description of solvent structure for the calculation of electron-transfer dynamics.

Before discussing the numerical methods for determining the hard-sphere pair distribution function or the accuracy of the hard-sphere potential itself, the procedures used to obtain the necessary parameters, such as the solvent diameter and packing fraction, are described. Any calculation of a hard-sphere distribution function requires the determination of an effective hard-sphere diameter, σ, related to the packing fraction η by

$$\eta = \pi\rho\sigma^3/6 \tag{11}$$

where ρ is the bulk solvent number density. For a given solvent of known density, the choice of σ (or η) is not obvious. A common approach is to model the solvent as a hard-sphere fluid with the same transport properties as the real liquid. This problem was initially formulated by Enskog, who extended Boltzmann's equation for dilute gases to describe the behavior of a dense, hard-sphere fluid.[48,73] A hard-sphere self-diffusion constant, D_{ens}, can be calculated from Enskog theory and is given by[73,74]

$$D_{ens} = \frac{3}{8\rho\sigma^2 g(\sigma)}\sqrt{\frac{kT}{\pi m}} \tag{12}$$

Here $g(\sigma)$ is the value of the pair distribution function at the contact distance, m is the hard-sphere mass (equal to the actual

molecular mass), and k is Boltzmann's constant. $g(\sigma)$ can be determined to a high degree of accuracy using the Carnahan−Starling equation of state:[48,75]

$$g(\sigma) = \frac{2 - \eta}{2(1 - \eta)^3} \tag{13}$$

When comparing diffusion constants from Enskog theory to those obtained from molecular dynamics simulations, Alder and Wainwright found it necessary to modify the Enskog result to account for correlated motion among the particles.[76,77] From fits to the Alder and Wainwright data, Czworniak et al. have suggested an approximate analytical form for the "correlated motion correction factor", C:[78]

$$C = 0.840 - 7.69(\eta - 0.463) - 32.3(\eta - 0.463)^2 \tag{14}$$

Using this correction factor as well as an additional factor to account for rotational−translational coupling,[58,78−80] given by the term A, the corrected hard-sphere self-diffusion constant, D, becomes

$$D = D_{ens}AC \tag{15}$$

Inclusion of the translational−rotational coupling factor, A, permits the theoretical hard-sphere diffusion constant to be compared to experimental diffusion constants for real liquids.[78−80] Comparison of the corrected Enskog result with several experimentally measured self-diffusion constants has led to excellent agreement for A values of 0.52.[78]

The corrected Enskog result given in eq 15 provides a method for calculating an effective hard-sphere diameter, σ. This diameter can then be used to generate a hard-sphere $g(R)$ using the methods detailed in section III.C. For solvents whose diffusion constants are known from experimental measurements, σ should be chosen so that eq 15 gives a diffusion constant in good agreement with experiment. This was the procedure used for cyclohexanone (CHX) for which an experimentally measured diffusion constant is reported in the literature.[81] However, for the other two solvents: dibutyl phthalate (DBP) and diethyl sebacate (DES), experimental values of the diffusion constants could not be found. In the absence of such information, the Spernol−Wirtz equation was used. Equations 8 and 15 were then solved self-consistently to find a hard-sphere diameter that led to agreement between the corrected Enskog and Spernol−Wirtz diffusion constants. To check the validity of this method, the same procedure was applied to find the hard-sphere diameter and packing fraction for CHX. It was found that the self-consistent procedure gave values which differed by only 0.5% from those obtained using the experimental diffusion constant. This helps confirm that the self-consistent approach provides an accurate determination of these required system parameters. To our knowledge, this is the only available approach for the determination of the hard-sphere diameter in the absence of experimental information.

C. Solvent Structure. In light of the significant role that solvent structure plays in the dynamics of electron transfer, it is important to use an accurate description of the radial distribution function. Fortunately, there has been a great deal of theoretical work done to model the two-particle rdf. While these calculations are constrained to systems of either hard-spheres or the softer Lennard-Jones potential, they provide excellent approximations of the local structure of many organic liquids. Due to the paucity of neutron-scattering data on complex organic liquids, these numerical techniques are generally the only means from which accurate $g(R)$ values can be obtained.

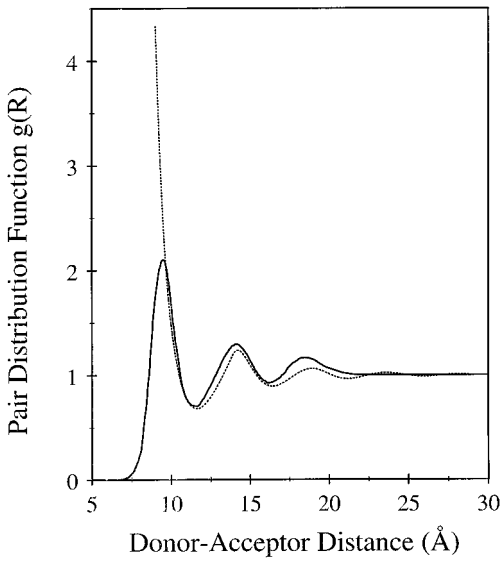

Figure 1. Radial distribution functions, $g(R)$, for benzene. The solid line is from ref 90 and shows the experimental $g(R)$ determined from neutron scattering. The dashed line is a calculated hard-sphere $g(R)$ from numerical solutions to the Percus−Yevick equation, using an effective hard-sphere diameter $\sigma = 4.98$ Å and packing fraction $\eta = 43.5\%$. Both the experimental and theoretical $g(R)$ curves for the pure solvent are shifted to a donor−acceptor contact distance of 9.0 Å.

A variety of methods have been developed to calculate $g(R)$ functions,[35,82−85] the most well-known of which was presented by Percus and Yevick (PY).[35,86] Solutions to the PY integral equation have allowed numerical calculations of $g(R)$ for solutions of hard-sphere particles[36,37,49,87] and for molecules interacting via a Lennard-Jones 6−12 potential.[88] Slight corrections to the hard-sphere rdf were obtained by Verlet and Weis,[89] with the results being found to agree quite well with experimental observations and simulations.

To examine the efficacy of modeling the solvent as hard spheres with a $g(R)$ given by solutions to the PY equation, model electron-transfer calculations of the excited state probability $\langle P_{ex}(t)\rangle$ were generated for donors and acceptors in benzene. This solvent was chosen because neutron diffraction studies have been carried out on this pure liquid, giving an experimentally determined radial distribution function.[90,91] Using the experimentally determined benzene $g(R)$, calculations of charge-separation dynamics were carried out for a wide variety of electron-transfer parameters, J_0 and β, and for different diffusion coefficients and acceptor concentrations. For comparison, $\langle P_{ex}(t)\rangle$ curves were also calculated using the identical system parameters, but with a numerically obtained hard-sphere $g(R)$ function. This hard-sphere $g(R)$ was generated using the Smith and Henderson PY algorithm with the correction of Verlet and Weis and a hard-sphere radius and packing fraction calculated with the methods of section III.B.

The experimental and calculated rdf curves are compared in Figure 1. The most significant discrepancy between the two functions is in the region just around contact, where, in general, the rates of electron transfer are the largest. The hard spheres have a well-defined distance of closest approach, while the real benzene liquid, having a softer potential, displays a $g(R)$ that goes smoothly to zero at short distance. However, the areas under the experimental and the hard-sphere $g(R)$ curves are virtually identical. The probability of two molecules being closer than "contact" in the experimental benzene $g(R)$ is made up for with increased density at contact in the hard-sphere case.

While the two forms of the rdf behave differently at contact, their structure is, in general, quite similar. These differences

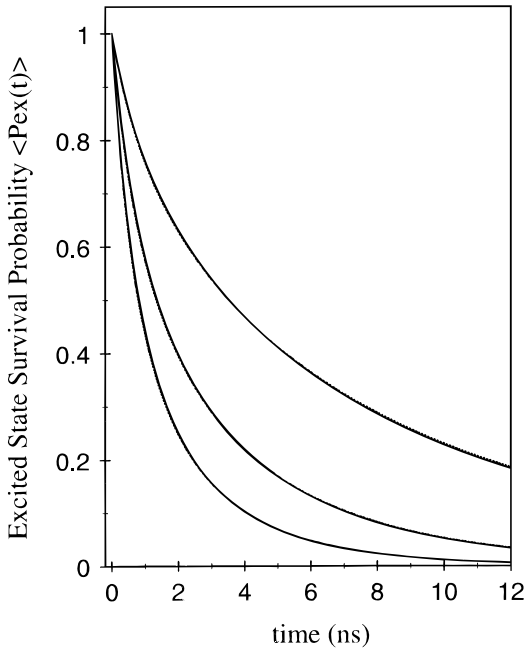

Figure 2. Excited-state survival probability $\langle P_{ex}(t)\rangle$ curves for three concentrations calculated using both the experimental and theoretical hard-sphere $g(R)$ from Figure 1. The figure demonstrates that the hard-sphere $g(R)$ is an excellent approximation to an experimental $g(R)$ in the forward electron-transfer calculations. Six curves are shown: a solid and dashed line for each concentration (0.1, 0.2, and 0.3 M), with the solid lines calculated using the experimental $g(R)$ and the dashed line from the theoretical hard-sphere $g(R)$. The solid lines were generated with electron-transfer parameters: $J_0 = 2.6$ cm^{-1}, $\beta = 0.67$ Å^{-1}, and the dashed lines are the best fits to these parameters, using a hard-sphere $g(R)$ and $J_0 = 2.7$ cm^{-1} and $\beta = 0.66$ Å^{-1}. The dielectric constants are $\epsilon_{op} = 2.2$ and $\epsilon_s = 6.4$, $\Delta\epsilon = 1.85$ eV, and $D = 12.0$ Å^2/ns.

were observed to play only a small role in the ensemble averaged kinetics of electron transfer. The very minor error introduced by using the hard-sphere $g(R)$ rather than the experimental form is displayed in Figure 2. The solid lines are $\langle P_{ex}(t)\rangle$ curves calculated using the experimental rdf, with parameters $J_0 = 2.6$ cm^{-1}, $\beta = 0.67$ Å^{-1}, $\Delta\epsilon = 1.85$ eV, $D = 12$ Å^2/ns, for three acceptor concentrations, 0.1, 0.2, and 0.3 M. The same calculations were made using the hard-sphere $g(R)$, and the resulting curves were found to differ by only a few percent. The J_0 and β values used in the hard-sphere calculation were then varied slightly to see whether different values would improve the agreement with the curves calculated from the experimental $g(R)$ and the original J_0 and β. The dashed lines in Figure 2 are the best fits, using the hard-sphere rdf and J_0 and β values of 2.7 cm^{-1} and 0.66 Å^{-1}, respectively, with all other system parameters held constant. The agreement in the $\langle P_{ex}(t)\rangle$ curves for all three concentrations using both forms of $g(R)$ is essentially exact, making the two sets indistinguishable. The electron-transfer parameters are virtually identical and are well within the uncertainty in the determination of these values in real experiments. This same behavior was reproduced for all values of the transfer parameters and acceptor concentrations that were studied. For any J_0 and β, the $\langle P_{ex}(t)\rangle$ curves calculated using either the experimental or theoretical hard-sphere $g(R)$ were very similar. In every case, by varying the transfer parameters a few percent or less, identical excited-state probability curves were obtained. These results confirm that the PY hard-sphere $g(R)$ provides an adequate representation of real liquid structure and is sufficiently accurate to warrant use in the calculation of electron-transfer parameters. In addition, this emphasizes the utility of the methods presented in section III.B for obtaining realistic values for the hard-sphere radius, σ, and the solvent packing fraction, η. Using widely available viscosity and density data for the solvents and crystallographic data for each solute, it is possible to calculate accurate values for the system properties necessary for analysis of electron-transfer experiments.

As mentioned above, the hard sphere $g(R)$ values were calculated using the inverse Laplace transform of Thiele's and Wertheims's solution to the PY equation.[35−38] An analytical formulation of these transforms has been published by Smith and Henderson.[87] These curves were then corrected according to the algorithm of Verlet and Weis.[89] It should be noted that these $g(R)$ calculations are for homogeneous solutions of pure solvent molecules. Wertheim has determined the Laplace transform solution to the PY equation for the case of a heterogeneous solution of different particles.[37] Throop and Bearman[88] investigated these solutions, and found that in the limit of low solute-to-solvent packing fraction ratio (less than 0.1, or about 1 mol/L), the solute molecules simply follow the one-component $g(R)$ created by the solvent molecules. For these cases of low-concentration solutes, the solute−solute $g(R)$ followed the high-density solvent $g(R)$, but the hard-sphere contact distance was given by the sum of the solute radii. These results can be used to simplify the work required to obtain accurate hard-sphere rdf curves for experimental electron-transfer systems. It is sufficiently accurate to calculate the one component $g(R)$, using the packing fraction and molecular diameter of the bulk solvent. The radial contact value is then set equal to the hard-sphere contact diameter of the donor and acceptor. If desired, it is possible to directly calculate $g(R)$ curves for heterogeneous solutions of mixed solutes and solvents.[38,49,88] A more complete discussion of the uses and limitations of $g(R)$ calculations has been presented previously.[34]

IV. Experimental Methods

A. Sample Preparation. The electron-donating chromophore is rubrene (RU), and the acceptor is duroquinone (DQ). This charge-transfer system was investigated in several solvents of varying viscosity and dielectric properties. In order of decreasing viscosity, the solvents used were dibutyl phthalate, diethyl sebacate, and cyclohexanone. RU in solution is readily oxidized in the presence of oxygen and light, and the sample preparation was developed accordingly.

All the reactants and solvents were filtered or purified prior to use. The acceptor, DQ, was sublimated twice. As RU is not easily sublimed or recrystallized, it was dissolved in the degassed solvent and then filtered (2 μm filter) in the dark. Each sample was prepared by serial dilution from stock solution. The RU concentrations were 10^{-4} M, while the DQ concentration varied from 0.05 to 0.33 M. Each solution was freeze−pump−thaw cycled five times with liquid nitrogen to further reduce the oxygen concentration. The final concentrations of DQ were determined spectroscopically at 430 nm, after first correcting for RU absorption at this wavelength. The extinction coefficient is $\epsilon_{430}^{DQ} = 27.2$ M^{-1}cm^{-1}.

The viscosities of the liquid solvents were measured using an Ubbelohde viscometer. The values were found to be independent of acceptor concentration. The high-frequency dielectric constant of each solvent, ϵ_{op}, was determined from the square of the index of refraction. These values were obtained using an Abbeé refractometer and agreed within error with published values. The low-frequency dielectric constant of DES, ϵ_s was found using a capacitance bridge. It was observed to be constant over the range of 120 Hz to 1 kHz and was independent of acceptor concentration. The value of ϵ_s for DBP and CHX were obtained from the literature.[92]

B. Time-Correlated Single-Photon Counting. The fluorescence lifetime of the photoexcited donor and lifetimes of donors quenched by forward electron transfer were measured by time-correlated single-photon-counting experiments (TCSPC). A synch-pumped dye laser, cavity dumped at 800 kHz, was pumped by a 41 MHz continuous-wave acoustooptically mode-locked and frequency-doubled Nd:YAG laser. Fluorescein 548 dye, base shifted with NaOH, was used to obtain lasing at 545−575 nm. The electron-transfer samples were excited with vertically polarized 552 nm pulses of approximately 10 ps duration. Using a front-face geometry, the fluorescence was collected by a lens and focused on the entrance slit of a subtractive double monochromator. The detection apparatus was polarized along the magic angle to remove decay of the fluorescence arising from rotational diffusion. All fluorescence frequencies to the red of 575 nm were passed by the monochromator and collected by a multichannel plate detector (Hamamatsu R2809-06). Narrow-band wavelength measurements to the red of 575 nm were made at several wavelengths, and there was no indication of a wavelength dependence of the time evolution of the fluorescence. The instrument response for each TCSPC fluorescence measurement was typically a 70 ps fwhm near-Gaussian line shape, with a tailing shoulder. The instrument response was measured with each data set and used for convolutions in the data analysis.

C. Measurements of Reaction Free Energies. The classical form of the Marcus theory distance-dependent electron-transfer rate constants, given in eqs 1 and 2, require knowledge of the free energy of reaction for each molecular system in each solvent being studied. Distance dependent values of $\Delta G(R)$ were calculated using the Rehm−Weller equation[44,45] (eq 3) and redox potentials were obtained by cyclic voltammetry. The energy of rubrene photoexcitation was taken to be 545 nm, the wavelength at which the normalized absorption and fluorescence spectra overlap.[93]

The oxidation and reduction potentials necessary for calculating ΔG were determined experimentally because literature values are not available for low dielectric solvents such as dibutyl phthalate (DBP) or diethyl sebacate (DES). Unlike polar solvents in which the free energy of reaction varies only slightly from one solvent to another, low dielectric constant solvents generally show much larger variations. Several theoretical methods of calculating the change in ΔG caused by transferring systems from one solvent to another have been proposed in the literature.[94,95] However, these methods give widely varying results. This was particularly true in the lower dielectric constant solvents, DBP and DES. As a result, it was necessary to perform cyclic voltammetry experiments to obtain the ΔG values.

Accurate experimental determination of redox potentials in low dielectric constant liquids is difficult for several reasons. At the extreme voltages necessary to measure redox potentials in low dielectric solvents, oxygen and water impurity signals are found to be a significant problem. Also, addition of electrolyte to nonpolar liquids can cause a premature rise in current compared to the pure solvent. Nonetheless, the experimentally determined values are expected to be substantially more accurate than values obtained from theoretical corrections to measurements performed in highly polar solvents.

Precautionary measures were taken to eliminate water and oxygen impurities in all the solvents. Each sample was placed over 4 Å activated molecular sieves for at least 24 h. All three solvents were freeze−pump−thawed on a vacuum line, sealed off, and opened in a glovebag under Ar. Experiments were performed using a Bioanalytical Systems 10 μm diameter Pt ultramicroelectrode and an Ensman 400 dual-electrode potentiostat in a two-electrode mode. The reference electrode was an Ag wire. The reverse processes of RU reduction and DQ oxidation did not interfere with the desired signals, so both species were put into solution simultaneously. This allowed the desired difference in redox potentials ($\Delta\epsilon = \epsilon^0$(RU,ox) − ϵ^0(DQ,red)) to be measured directly. As a supporting electrolyte, the salt tetrahexylammonium perchlorate (Fluka) was used as received. Typical salt concentrations were between 1 and 30 mM. Decreasing the salt concentration by a factor of 10 was found to have no effect on the measured potentials. The typical concentrations of the redox species were 0.1 mM.

Sigmoidal steady-state plots were taken for all three solvents. The solvents with higher dielectric constants, DBP and CHX, provided precise, reproducible ΔG values. The solvent with the lowest dielectric constant, DES, was more difficult to measure, and the results were somewhat less reproducible. In addition, an *IR* drop was observed in DES, and the results were mathematically corrected. The error in ΔG was ±0.02 eV for CHX and DBP and ±0.1 eV for DES.

TABLE 1: Parameters Used To Analyze the Electron-Transfer Data in Each Solvent[a]

	η (%)	σ (Å)	D (Å^2/ns)	ϵ_{op}	ϵ_s	$\Delta\epsilon$ (eV)	τ (ns)
DBP	54.0	7.70	13.2	2.2	6.4	1.85	15.5
DES	53.0	7.67	41.5	2.07	5.0	2.1	15.1
CHX	50.0	5.48	97.2	2.1	18.3	1.82	14.7

[a] DBP, dibutyl phthalate; DES, diethyl sebacate; CHX, cyclohexanone. η, hard sphere packing fraction; σ, hard sphere diameter; D, diffusion constant; ϵ_{op}, high-frequency dielectric constant; ϵ_s, static dielectric constant; $\Delta\epsilon$, difference between RU and DQ redox potentials; τ is the rubrene fluorescence lifetime.

V. Results

Using the theory presented above, with appropriate values for the system parameters discussed in section III, fits were obtained for the time-dependent fluorescence quenching measurements of RU and DQ in the three solvents. Values of the through-solvent electron-transfer parameters, J_0 and β, were determined by comparison of the $\langle P_{ex}(t)\rangle$ calculations, convolved with a measured instrument response, to TCSPC fluorescence measurements. Several acceptor concentrations were studied in each solvent. The best fit to each experimental curve was determined by a least-squares fitting routine, using the downhill simplex method of parameter optimization.[55,96] To the extent that the classical form of the Marcus rate coefficient (eq 1) provides a full description of solute and solvent energies of reaction, the two parameters J_0 and β are expected to have reasonably consistent values for electron transfer between the same donor and acceptor in any solvent.

In addition to the electron transfer parameters, there are a variety of system parameters needed to fit the data. These are given in Table 1. The free energy of reaction at each separation distance, R, was calculated from the difference in redox potential, $\Delta\epsilon$, obtained from cyclic voltammetry measurements described above. The Fick mutual diffusion coefficient between RU and DQ was calculated using the measured viscosity at 25 °C, with the Spernol−Wirtz correction to the Stokes−Einstein equation.[65] The radiative lifetime, τ, of photoexcited rubrene in each solvent was found by least-squares fit of a single-exponential decay to fluorescence measurements taken in the absence of duroquinone. These decays were observed to be single exponentials over the full time scale of the experiment, more than 5 lifetimes of RU in each solvent. The radial distribution functions, $g(R)$, were obtained using solutions to the Percus−Yevick equations, with corrections due to Verlet

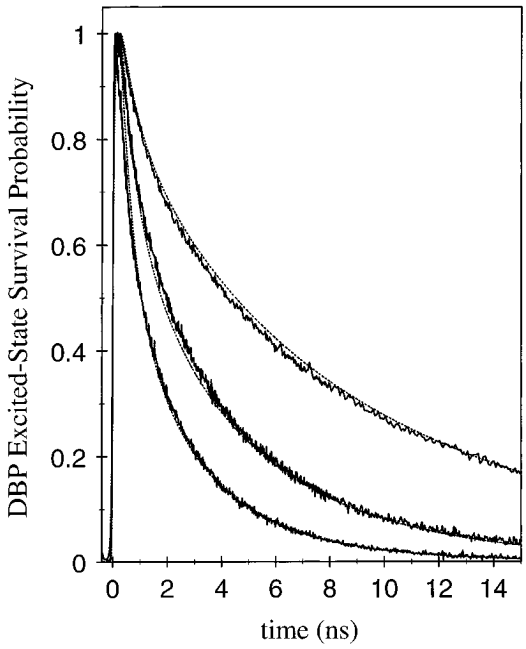

Figure 3. Fluorescence quenching RU/DQ data in the solvent DBP, with best-fit $\langle P_{ex}(t)\rangle$ calculations. Three samples with different DQ concentrations were studied experimentally, 0.11, 0.22, and 0.33 M, with the highest concentration showing the fastest decay. The best-fit parameters are $J_0 = 3.1$ cm^{-1} and $\beta = 0.6$ Å^{-1} for a diffusion constant of 13.2 Å^2/ns, with a donor−acceptor contact distance of 7.9 Å. Additional parameters are given in Table 1.

and Weis. These were calculated for systems of a homogeneous solvent, with molecular diameters and packing fractions obtained via the self-consistent method detailed in section IIIB.

The fluorescence quenching data of RU and DQ in each solvent is presented with the fluorescence lifetime removed, in order to more directly examine the process of electron transfer. This was accomplished by dividing each decay by a single exponential, obtained as a fit to the fluorescence decay of pure RU in each solvent. The resulting files were then fit with calculated $\langle P_{ex}(t)\rangle$ functions, each convolved with the measured instrument response. Removing the contribution of the fluorescence lifetime decay from the data allowed a more direct comparison of the transfer dynamics for each acceptor concentration but did not affect the choice of electron-transfer parameters or the quality of the theoretical fits. This was particularly useful for the higher viscosity solvents and lower acceptor concentration samples, in which fluorescence plays a significant role in the measured excited-state decay.

Figure 3 shows fluorescence quenching data of rubrene for three concentrations of duroquinone in the solvent DBP. The dashed lines are the best fits for each decay, as determined by the method of minimization of least squares. All three concentrations, 0.11, 0.22, and 0.33 M, were fit simultaneously to obtain a single χ^2 value used in the least-squares minimization. The electron-transfer parameters for the best fit are $J_0 = 3.1$ cm^{-1} and $\beta = 0.6$ Å^{-1}. For given values of all the required system parameters, such as $\Delta\epsilon$, D, σ, and η, the J_0 and β given above were found to be the only transfer parameters which correctly modeled the data. Estimation of the error bars on these Marcus constants were obtained by varying the experimental system parameters within the limits of their uncertainties. For a particular set of values of all the system parameters, such as those given in Table 1, it was found that the best fit value of J_0 and β were very precisely determined, with a variation in each of less than ± 0.05. However, if the system parameters, i.e., $\Delta\epsilon$, D, σ, and η, were varied, the observed best fit values of J_0 and β were again precisely determined, although the error bars could be as large as ± 0.3 for J_0 and ± 0.1 for β.

An important point to note about the values and error bars on J_0 and β is that for any given choice of all the system parameters within the error bars of each, the sharp uniqueness of the transfer parameters in DBP was always observed. In all cases, only one particular set of values of the Marcus parameters J_0 and β fit the experimental decays accurately. Thus, for electron transfer between RU and DQ in this solvent, the distance dependence and magnitude of through-solvent electron transfer is well defined by these parameters. However, although the fits are unique, the determination of J_0 and β relies on accurate knowledge of the solvent structure, the form of the hydrodynamic effect, and the diffusion constants. These physical parameters may be difficult to obtain for a real molecular liquid, and a contribution to the J_0 and β error bars is thus expected due to the extreme difficulty of calculating these quantities accurately for a complex molecular system. Nevertheless, the theory presented here is the first to incorporate a realistic description of solvent and hydrodynamic effects in a detailed treatment of intermolecular electron transfer. The J_0 and β values reported here should be substantially more accurate than values determined from fits which treat the liquid as a featureless continuum. For molecular reactions in the Marcus normal region, the dependence of the transfer rate on particle separation is generally observed to be an exponential decay. This falloff in transfer rate is specified in large part by the parameter β, as given in eq 1. By uniquely determining the values of the Marcus rate parameters, the distance dependence of charge transfer between RU and DQ in the solvent DBP is well defined. The functional form of $k_f(R)$ indicates that molecules with 2−3 Å edge-to-edge separation are highly involved in the electron-transfer process, and even molecules with a 6 Å separation have a reasonable probability of reacting. This emphasizes the fact that rather than occurring only at molecular contact, electron-transfer reactions involve noncontact, solvent-separated molecules.

The ability of the theory to fit the data with a unique pair of transfer parameters was influenced by the viscosity of the solvent. It has been observed in previous experiments analyzed with the continuum theory[4] that for systems with large mutual diffusion rates, it is not possible to uniquely determine values for J_0 and β. Instead, as was observed in the present experiments for the two low-viscosity solvents, a range of pairs of electron-transfer parameters is found to fit the experimental data equally well. Although the DBP fits were unique, the range of parameters capable of fitting the data increased for the solvents DES and CHX, which have progressively larger diffusion coefficients. The reason behind this trend can be qualitatively understood from the following argument. In the limit of infinite diffusion, every microstate of the electron-transfer system (one donor surrounded by many acceptors, in a volume large enough to effectively represent an infinite system on the time scale of electron-transfer events) experiences an identical probability distribution of acceptor particles. Each donor no longer sees a unique acceptor configuration but rather sees a static configuration given by $p'(R)$, which is identical for every donor. Thus, rather than having to average over all possible microstates of the ensemble to obtain the observable $\langle P_{ex}(t)\rangle$, each microstate is a representation of the ensemble average. In this case of infinite diffusion rates, the functional form of the rate coefficient, $k_f(R)$, becomes unimportant. Instead, the only relevant feature is the spatial integral:[97]

$$C\int_{R_m}^{\infty} k_f(R)\, p'(R)\, dR \qquad (16)$$

Equation 16 defines an effective "reactive density," and in the limit of infinite diffusion, the decay of the excited-state probability is a simple exponential with a decay constant given by eq 16. It is clear that in this case, the values of the individual parameters J_0 and β are no longer unique and separable. All that is important is the choice of the two parameters simultaneously, such that the integral of eq 16 gives the appropriate value. There are many functional forms of $k_f(R)$ which can be sufficient to give the correct exponential decay, and thus many different pairs of J_0 and β (chosen simultaneously) can be adequate.

While this behavior does not rigorously hold for large, but less than infinite, values of the diffusion coefficient, similar results are observed. The uniqueness of the choice for the transfer variables was related to the inverse of the magnitude of D. Excellent theoretical fits to the fluorescence quenching data in DES and CHX were found, but more than one pair of J_0 and β is capable of fitting the data. For the moderate viscosity solvent, DES, it was possible to find sets of the two transfer parameters which fit the data with a range in β between 0.3 and 1.0 Å^{-1}. For all values of β within this range, there was a corresponding unique value of J_0. For values outside this range, it was not possible to find any pair of the parameters which fit the data. For the least viscous solvent, CHX, there were few limitations on the magnitude of the parameters. For any value of β greater than 0.2 Å^{-1}, a single value of J_0 could be found which could provide an excellent fit to the data.

While the rates of diffusion for both DES and CHX are not infinite, they are, on the time scale of typical through-solvent electron-transfer events, quite fast. This leads to a complex interplay between the magnitude of D, the functional form of $k_f(R)$, and the value of the integral given by eq 16. For intermediate values of D, various pairs of J_0 and β fit the data, but these do not give rise to identical values of the reactive density. Rather, there is a moderate range of values of the reactive density that give appropriate $\langle P_{ex}(t)\rangle$ curves. As D becomes larger, such as for CHX, the dependence on the form of $k_f(R)$ is further lessened. This results in a smaller spread in the values of the reactive density which are capable of producing the correct excited-state decay. At the same time, it becomes more likely that any choice of J_0 and β which gives the proper value of the reactive density will fit the data, regardless of the functional form of $k_f(R)$.

This behavior makes it impossible to determine independent values of J_0 and β in very low viscosity solvents. However, following the concepts of Marcus theory, the distance dependence of through-solvent transfer for the same donor−acceptor pair is expected to be similar in any solvent. This distance dependence is largely governed by the magnitude of β, while J_0 acts as an amplitude factor. For this reason, the magnitude of β obtained in the highest viscosity solvent, DBP was used in the calculations of the data taken in DES and CHX. Figures 4 and 5 display the best fits to the data in DES and CHX, respectively, with β fixed at 0.6 Å^{-1}. The optimal choice of J_0 is 5.8 and 7.8 cm^{-1} in the two solvents, respectively. The acceptor concentrations were 0.11, 0.22, and 0.30 M in DES and 0.056, 0.11, and 0.22 M in CHX. In the limit that eqs 1 and 2 fully represent all the solvent and molecular interactions inherent in through-solvent electron transfer, the magnitude of J_0 is expected to be similar in each solvent. The J_0 values obtained for these three solvents are relatively close. If β is allowed to vary a small amount, then J_0 values can be brought into closer agreement. Due to the possible errors in the magnitudes of the input parameters, e.g., the diffusion constants

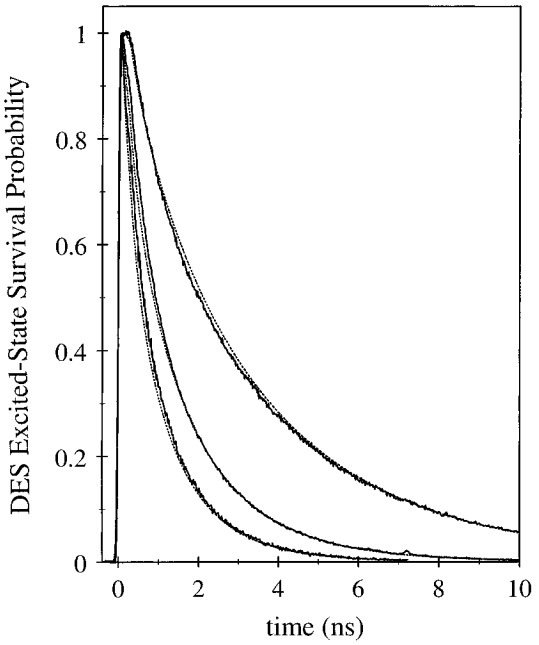

Figure 4. Fluorescence quenching data and best fits to the excited-state decay of the RU/DQ system in DES. The DQ concentrations are 0.11, 0.22, and 0.30 M, and the electron transfer parameters are $J_0 = 5.8$ cm^{-1} and $\beta = 0.6$ Å^{-1}. The system parameters are given in Table 1.

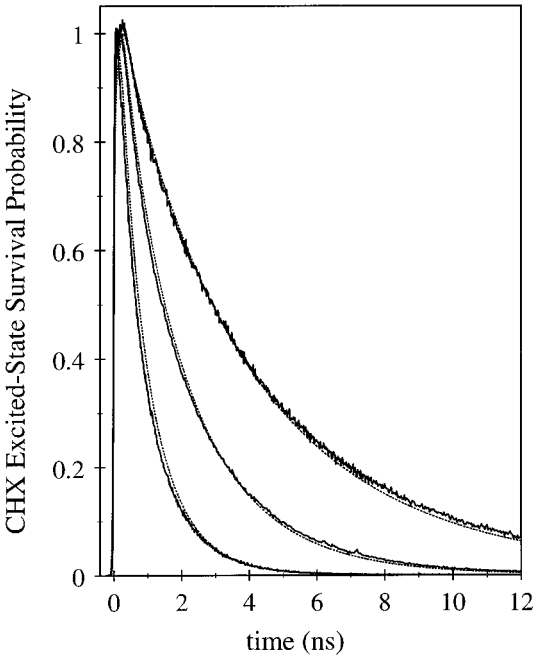

Figure 5. Data and best fits to the excited-state decay of the RU/DQ system in CHX. The DQ concentrations are 0.056, 0.11 and 0.22 M, and the electron-transfer parameters are $J_0 = 7.8$ cm^{-1} and $\beta = 0.6$ Å^{-1}. The system parameters are given in Table 1.

and the rdfs, it is not possible to determine if the small differences in the J_0 and β values needed to fit the data in the three solvents are real. However, it is possible that some factors which have been studied as extensions to Marcus theory play a role in the dynamics of the rubrene−duroquinone system. For example, contributions from single-mode or multimode vibrational solvent coupling[29,98,99] may influence the transfer rate in a manner that depends on the detailed molecular nature of the solvent. These theoretical refinements can be included in calculations of electron-transfer observables with only minor changes to the mathematical methods described above.

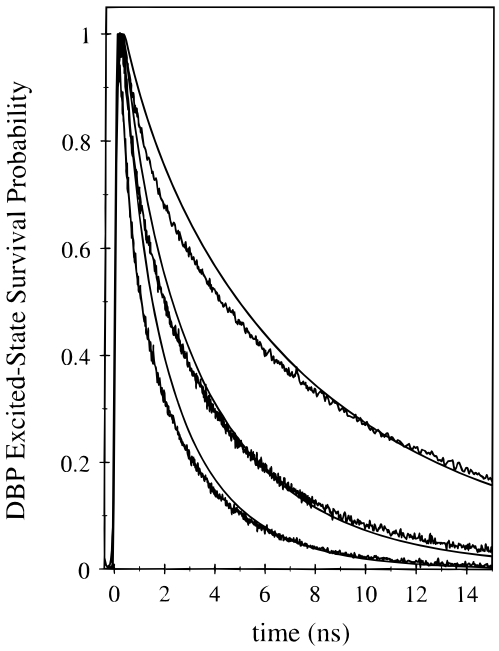

Figure 6. Data and best fits to the excited-state decay of RU/DQ in DBP, using the simple theoretical model with no solvent structure effects included. This demonstrates the inability of the uncorrected model to fit some experimental systems. The best fit Marcus parameters are $J_0 = 7.8$ cm^{-1} and $\beta = 1.9$ Å^{-1}. All other system parameters are identical to those given in Figure 3.

As a final check, it is important to examine the necessity of including the physical corrections presented in this paper to the statistical mechanical model. The basic form of the theory, without including the effects of solvent structure and hydrodynamic effect, has previously been used to examine and analyze a number of experimental electron-transfer systems.[4,32,100] However, as discussed above, the results obtained from this analysis may incorrectly skew the values of the Marcus parameters to account for the solvent effects which have been ignored up to this point. A full comparison of the theoretical methods which take these corrections into account to the original uncorrected form has been presented recently.[34] Most important, however, is the quality with which the simple continuum solvent form of the model can fit the reaction dynamics in highly viscous solvents. Figure 6 presents the fluorescence quenching measurements of rubrene and duroquinone in DBP, with the best fits which could be obtained from the uncorrected form of the theoretical model. The data is the same as Figure 3, and thus the quality of the fits can be directly compared to those obtained using the full theory including solvent structure and diffusion effects. The best fits for the uncorrected model, as measured by least-squares minimization, were obtained for the Marcus parameters $J_0 = 7.8$ cm $^{-1}$ and $\beta = 1.9$ Å^{-1}. It is clear that not only is the simple form of the model unable to adequately fit the excited state observable in this solvent, but the parameters found for these fits were fundamentally different from the values obtained using the full form of the theory. The inability of the continuum solvent expressions to reproduce the experimental data was most pronounced for the most viscous solvent, DBP. For the more rapidly diffusing systems, DES and CHX, the simple form of the theory was able to produce somewhat closer fits to the measured data. However, it was observed for these cases as well, that the best-fit Marcus parameters were found to again be drastically different from those obtained using the detailed calculation of $\langle P_{ex}(t)\rangle$. These results further emphasize the importance of including the solvent structure details in the theory as discussed in this paper.

VI. Concluding Remarks

This paper presents the first comprehensive analysis of photoinduced electron transfer in liquids which correctly accounts for the important effects of solvent structure and distance-dependent diffusion rates. While earlier theoretical and experimental studies have examined the through-solvent behavior and dynamics of intermolecular charge transfer in liquids,[11,14−16,22,24−26] the serious theoretical issues introduced by the finite volume of solvent molecules have not been included in previous experimental studies and have only recently been treated theoretically.[34]

For a donor surrounded by many acceptors in a liquid, a key component in understanding the dynamics of photoinduced electron transfer in liquids is the spatial distribution of the acceptors. This includes both the initial distribution and the change in acceptor positions with time due to diffusion. For studies in which the distance between the donor and a single acceptor is fixed by chemical linkage, the difficulties associated with time varying spatial distribution of acceptors in a liquid is avoided. However, the questions that are addressed are also fundamentally different. At a single fixed distance, it is only possible to measure a single value for the transfer rate constant. The important parameters in the Marcus theory, J_0 and β, cannot be determined independently. Furthermore, the transfer rate constant that is measured for a linked donor−acceptor system arises in part, or can be dominated by, through-bond interactions. If the linkage is made longer to examine the distance dependence of the transfer rate, it is unclear how the change in the distance plays off against the change in the nature of the linkage between the donor and acceptor. Therefore, while linked systems can provide important information on electron transfer, they cannot fully address the nature of through-solvent transfer for donors and acceptors that are not covalently coupled.

The experimental and theoretical techniques presented above provide the most complete methods currently available for obtaining values of the Marcus transfer parameters, J_0 and β, for through-solvent electron transfer. Inclusion of the solvent structure via the pair distribution function and incorporation of a distance-dependent diffusion constant gives a much more realistic description of the solvent than treatments which ignore these effects. The rate parameters reported here are thus expected to be the most accurate determined to date for intermolecular electron transfer in liquids. However, these results are contingent upon detailed knowledge of system parameters such as the radial distribution function. Future work will focus on obtaining these parameters more accurately. Additionally, work is currently in progress analyzing the ion kinetics from pump probe data.[101] The ion kinetics provide an additional check of the reliability of the forward transfer parameters. This occurs because successful analysis of the ion state probability requires a detailed knowledge of the ion distribution created by forward transfer. Thus, pump−probe experiments measuring ion recombination provide both information on the dynamics of geminate recombination and also an independent verification of the forward transfer analysis.

In general, it should be noted that the success and utility of the detailed electron-transfer theory have been well demonstrated by the fluorescence quenching measurements presented here. The inclusion of solvent structure and hydrodynamic effects have led to successful fits of the forward transfer kinetics for rubrene and duroquinone in several solvents. The dynamics of charge separation in the highest viscosity solution, DBP, was uniquely specified by a well-defined pair of the transfer parameters. The measured value of $\beta = 0.6$ Å^{-1} is smaller than commonly cited values of roughly 1.0 Å^{-1}. However,

previous studies in liquids do not take the necessary solvent effects into account, and covalently linked systems measure through-bond charge separation rather than through-space transfer.

The interesting behavior seen in the limit of fast diffusion suggests further avenues of study in charge separation reactions. Although the values for J_0 and β may not be able to be determined independently in low-viscosity solvents without additional study of higher viscosity solvents simultaneously, information on the kinetics is still available. As the mutual diffusion coefficient becomes large, the reactive density (given by eq 16) becomes the identifiable parameter. Since the reactive density should exhibit a direct dependence on ΔG, free energy studies may be more straightforward to accomplish in low-viscosity solvents.

Finally, it is important to recognize that the study of electron transfer among molecules freely diffusing in liquids or in other types of systems, such as micelles,[102] goes beyond trying to determine the underlying molecular electron-transfer parameters. Photoinduced electron-transfer redox chemistry in bulk systems is an area of chemistry that can play an important role in solar energy conversion. The major goal is to produce long-lived charge separation so that the highly reactive radical ions may go on to do useful chemistry. The experiments and theory described in this paper provide insights into the complex kinetics that occur in electron-transfer systems in solution. In a subsequent publication,[101] the same types of theoretical considerations will be applied to experimental studies of geminate recombination following photoinduced electron-transfer. An understanding of the interplay of the many processes influencing charge separation may lead to the ability to design useful photochemical redox systems.

Acknowledgment. We would like to thank Professor Hans C. Andersen, Department of Chemistry, Stanford University, for a great many valuable discussions concerning liquid structure and the applicability of liquid structure theoretical methods to real liquids. We would also like to thank Professor Christopher E. D. Chidsey, Department of Chemistry, Stanford University, for allowing us to use his cyclic voltammetry equipment and for a great deal of help in performing the cyclic voltammetry measurements. We would also like to acknowledge Professor Nathan Lewis, Chemistry Department, California Institute of Technology, for useful suggestions concerning the cyclic voltammetry measurements. This work was supported by the Department of Energy, Office of Basic Energy Sciences (Grant DE-FG03-84ER13251). H.L.T. thanks the Office of Naval Research for a graduate fellowship. The computers used in this work were provided by a departmental grant from the National Science Foundation (Grant NSF-CHE-9408185).

References and Notes

(1) Huddleston, R. K.; Miller, J. R. *J. Phys. Chem.* **1982**, *86*, 200.
(2) Siders, P.; Cave, R. J.; Marcus, R. A. *J. Chem. Phys.* **1984**, *81*, 5613.
(3) Strauch, S.; McLendon, G.; McGuire, M.; Guarr, T. *J. Phys. Chem.* **1983**, *87*, 3579.
(4) Murata, S.; Matsuzaki, S. Y.; Tachiya, M. *J. Phys. Chem.* **1995**, *99*, 5354.
(5) Wynne, K.; Galli, C.; Hochstrasser, R. M. *J. Chem. Phys.* **1994**, *100*, 4797.
(6) Simon, J. D.; Su, S. *J. Chem. Phys.* **1987**, *87*, 7016.
(7) Shand, M. A.; Rodgers, M. A. J.; Webber, S. E. *Chem. Phys. Lett.* **1991**, *177*, 11.
(8) Eads, D. D.; Dismer, B. G.; Fleming, G. R. *J. Chem. Phys.* **1990**, *93*, 1136.
(9) Miller, J. R.; Peeples, J. A.; Schmitt, M. J.; Closs, G. L. *J. Am. Chem. Soc.* **1982**, *104*, 6488.
(10) Gould, I. R.; Young, R. H.; Moody, R. E.; Farid, S. *J. Phys. Chem.* **1991**, *95*, 2068.
(11) Inokuti, M.; Hirayama, F. *J. Chem. Phys.* **1965**, *43*, 1978.
(12) McConnell, H. *J. Chem. Phys.* **1961**, *35*, 508.
(13) Smoluchowski, M. V. *Z. Physik. Chem. (Leipzig)* **1917**, *92*, 129.
(14) Collins, F. C.; Kimball, G. E. *J. Colloid Sci.* **1949**, *4*, 425.
(15) Agmon, N.; Szabo, A. *J. Chem. Phys.* **1990**, *92*, 5270.
(16) Marcus, R. A. *Annu. Rev. Phys. Chem.* **1964**, *15*, 155.
(17) Beratan, D. N. *J. Am. Chem. Soc.* **1986**, *108*, 4321.
(18) Siders, P.; Marcus, R. A. *J. Am. Chem. Soc.* **1981**, *103*, 748.
(19) Brunschwig, B. S.; Ehrenson, S.; Sutin, N. *J. Am. Chem. Soc.* **1984**, *106*, 6858.
(20) Kestner, N. R.; Logan, J.; Jortner, J. *J. Phys. Chem.* **1974**, *78*, 2148.
(21) Yan, Y. J.; Sparpaglione, M.; Mukamel, S. *J. Phys. Chem.* **1988**, *92*, 4842.
(22) Lin, Y.; Dorfman, R. C.; Fayer, M. D. *J. Chem. Phys.* **1989**, *90*, 159.
(23) Dorfman, R. C.; Lin, Y.; Fayer, M. D. *J. Phys. Chem.* **1990**, *94*, 8007.
(24) Dorfman, R. C. Doctoral Thesis, Stanford University, 1992.
(25) Burshtein, A. I. *Chem. Phys. Lett.* **1992**, *194*, 247.
(26) Burshtein, A. I.; Zharikov, A. A.; Shokhirev, N. V. *J. Chem. Phys.* **1992**, *96*, 1951.
(27) Barbara, P. F.; Walker, G. C.; Smith, T. P. *Science* **1992**, *256*, 975.
(28) Guarr, T.; McLendon, G. *Coord. Chem. Rev.* **1985**, *68*, 1.
(29) Cortes, J.; Heitele, H.; Jortner, J. *J. Phys. Chem.* **1994**, *98*, 2527.
(30) Fayer, M. D.; Song, L.; Swallen, S. F.; Dorfman, R. C.; Weidemaier, K. In *Ultrafast Dynamics of Chemical Systems*; Simon, J. D., Ed.; Kluwer Academic Publishers: Amsterdam, 1994; p 37.
(31) Song, L.; Dorfman, R. C.; Swallen, S. F.; Fayer, M. D. *J. Phys. Chem.* **1991**, *95*, 3454.
(32) Song, L.; Swallen, S. F.; Dorfman, R. C.; Weidemaier, K.; Fayer, M. D. *J. Phys. Chem.* **1993**, *97*, 1374.
(33) Marcus, R. A. *J. Chem. Phys.* **1956**, *24*, 966.
(34) Swallen, S. F.; Weidemaier, K.; Fayer, M. D. *J. Chem. Phys.* in press.
(35) Percus, J. K.; Yevick, G. Y. *Phys. Rev.* **1958**, *120*, 1.
(36) Thiele, E. *J. Chem. Phys.* **1963**, *39*, 474.
(37) Wertheim, M. S. *Phys. Rev. Lett.* **1963**, *10*, 321.
(38) Lebowitz, J. L. *Phys. Rev.* **1964**, *133A*, 895.
(39) Rice, S. A. *Diffusion-Limited Reactions*; Elsevier: Amsterdam, 1985.
(40) Zwanzig, R. *Adv. Chem. Phys.* **1969**, *15*, 325.
(41) Deutch, J. M.; Felderhof, B. U. *J. Chem. Phys.* **1973**, *59*, 1669.
(42) Wolynes, P. G.; Deutch, J. M. *J. Chem. Phys.* **1976**, *65*, 450.
(43) Northrup, S. H.; Hynes, J. T. *J. Chem. Phys.* **1979**, *71*, 871.
(44) Rehm, D.; Weller, A. *Isr. J. Chem.* **1970**, *8*, 259.
(45) Fox, M. A. *Top. Curr. Chem.* **1991**, *159*, 67.
(46) Hansen, J. P.; McDonald, I. R. *Theory of Simple Liquids*; Academic Press, Inc.: London, 1976.
(47) Allen, M. P.; Tildesley, D. J. *Computer Simulation of Liquids*; Clarendon Press: Oxford, 1987.
(48) McQuarrie, D. A. *Statistical Mechanics*; Harper & Row: New York, 1976.
(49) Throop, G. J.; Bearman, R. J. *J. Chem. Phys.* **1965**, *42*, 2408.
(50) Swallen, S. F.; Weidemaier, K.; Fayer, M. D. *J. Phys. Chem.* **1995**, *99*, 1856.
(51) Williamson, B.; La Mer, V. K. *J. Am. Chem. Soc.* **1948**, *70*, 717.
(52) Noyes, R. M. *J. Am. Chem. Soc.* **1956**, *77*, 5486.
(53) Tachiya, M. *Radiat. Phys. Chem.* **1983**, *21*, 167.
(54) Agmon, N.; Hopfield, J. J. *J. Chem. Phys.* **1983**, *78*, 6947.
(55) Press, W. H.; Flannery, B. P.; Teukolsky, S. A.; Vetterling, W. T. *Numerical Recipes in C*; Cambridge University Press: Cambridge, 1988.
(56) Pines, E.; Huppert, D.; Agmon, N. *J. Chem. Phys.* **1988**, *88*, 5620.
(57) Andersen, H. C.; Chandler, D.; Weeks, J. D. *Adv. Chem. Phys.* **1976**, *34*, 105.
(58) Chandler, D.; Weeks, J. D.; Andersen, H. C. *Science* **1983**, *220*, 787.
(59) Ben-Amotz, D.; Herschbach, D. R. *J. Phys. Chem.* **1990**, *94*, 1038.
(60) Bondi, A. *J. Phys. Chem.* **1964**, *68*, 441.
(61) Birks, J. B. *Photophysics of Aromatic Molecules*; Wiley-Interscience: London, 1970.
(62) Marcus, A. H.; Fayer, M. D.; Curro, J. G. *J. Chem. Phys.* **1994**, *100*, 9156.
(63) Wolynes, P. G. In *Annu. Rev. Phys. Chem.* **1980**, *31*, 345.
(64) Ulstrup, J. *Charge Transfer Processes in Condensed Media*; Springer: Berlin, 1979; p 417.
(65) Spernol, A.; Wirtz, K. *Z. Naturforsch. Teil A* **1953**, *89*, 522.
(66) Sandhu, *J. Magn. Reson.* **1975**, *17*, 34.
(67) Terazima, M.; Okamoto, K.; Hirota, N. *J. Chem. Phys.* **1995**, *102*, 2506.
(68) Zwanzig, R. *J. Chem. Phys* **1970**, *53*, 3625.
(69) Hubbard, J.; Onsager, L. *J. Chem. Phys.* **1977**, *67*, 4850.

(70) Kennard, O.; Watson, D. G.; Rodgers, J. R. *Crystal Data Determinative Tables*, 3rd ed.; U.S. Department of Commerce, National Bureau of Standards and the JCPDS International Center for Diffraction Data: 1978.
(71) Wyckoff, R. W. G. *Crystal Structures*; Interscience Publishers: New York, 1969; Vol. 6.
(72) (a) For organic compounds whose rdf's have been measured experimentally and whose hard-sphere radii are known (e.g., benzene or naphthalene), the calculated radii from taking 74% of the crystallographic volume give values 10−20% too high. (b) Andersen, H., personal communication.
(73) Chapman, S.; Cowling, T. G. *The Mathematical Theory of Non-Uniform Gases*; Cambridge University Press: Cambridge, 1970.
(74) Protopapas, P.; Andersen, H. C.; Parlee, N. A. D. *J. Chem. Phys.* **1973**, *59*, 15.
(75) Protopapas, P.; Andersen, H. C.; Parlee, N. A. D. *Chem. Phys.* **1975**, *8*, 17.
(76) Alder, B. J.; Wainwright, T. E. *Phys. Rev. Lett.* **1967**, *18*, 988.
(77) Alder, B. J.; Gass, D. M.; Wainwright, T. E. *J. Chem. Phys.* **1970**, *53*, 3813.
(78) Czworniak, K. J.; Andersen, H. C.; Pecora, R. *Chem. Phys.* **1975**, *11*, 451.
(79) Chandler, D. *J. Chem. Phys.* **1974**, *60*, 3500.
(80) Chandler, D. *J. Chem. Phys.* **1974**, *60*, 3508.
(81) Claessens, M.; Fiasse, P.; Fabre, O. *Nouv. J. Chim.* **1984**, *8*, 357.
(82) Born, M.; Green, M. S. *A General Kinetic Theory of Liquids*; Cambridge University Press: Cambridge, 1949.
(83) van Leeuwen, J. M. J.; Groeneveld, J.; de Boer, J. *Physica* **1959**, *25*, 792.
(84) Meeron, E. *J. Math. Phys.* **1960**, *1*, 192.
(85) Verlet, L. *Nuovo Cim.* **1960**, *18*, 77.
(86) Percus, J. K. *Phys. Rev. Lett.* **1962**, *8*, 462.
(87) Smith, W. R.; Henderson, D. *Mol. Phys.* **1970**, *19*, 411.
(88) Throop, G. J.; Bearman, R. J. *J. Chem. Phys.* **1966**, *44*, 1423.
(89) Verlet, L.; Weil, J. J. *Phys. Rev. A* **1972**, *5*, 939.
(90) Misawa, M.; Fukunaga, T. *J. Chem. Phys.* **1990**, *93*, 3495.
(91) Ung Van, D.; Sandor, L. *Magyar Kem. Folyolrat* **1975**, *81*, 436.
(92) Riddick, J. A.; Bunger, W. B. *Organic Solvents: Physical Properties and Methods of Purification;* 3rd ed.; John Wiley & Sons: New York, 1970; Vol. II, p 1041.
(93) Bolton, J. R.; Archer, M. D. In *Electron Transfer in Inorganic, Organic, and Biological Systems*; Bolton, J. R., Mataga, N., McLendon, G., Eds.; The American Chemical Society: Washington, 1991; p 9.
(94) Weller, A. *Z. Phys. Chem. N.F.* **1982**, *133*, 93.
(95) Vanthey, E.; Phillips, D. *Chem. Phys.* **1990**, *147*, 421.
(96) Nelder, J. A.; Mead, R. *Comput. J.* **1965**, *7*, 308.
(97) Marcus, R. A.; Siders, P. *J. Phys. Chem.* **1982**, *86*, 622.
(98) Asahi, T.; Ohkohchi, M.; Matsusaka, R.; Mataga, N.; Zhang, R. P.; Osuka, A.; Maruyama, K. *J. Am. Chem. Soc.* **1993**, *115*, 5665.
(99) Bixon, M.; Jortner, J.; Cortes, J.; Heitele, H.; Michel-Beyerle, M. E. *J. Phys. Chem.* **1994**, *98*, 7289.
(100) Dorfman, R. C.; Lin, Y.; Fayer, M. D. *J. Phys. Chem.* **1989**, *93*, 6388.
(101) Weidemaier, K.; Swallen, S. F.; Tavernier, H. L.; Fayer, M. D., in press.
(102) Weidemaier, K.; Fayer, M. D. *J. Phys. Chem.* **1996**, *100*, 3767.

JP953583L